MATHEMATICS CLINIC

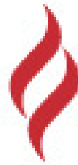

Claremont

GRADUATE UNIVERSITY

****

Quantum Corrections to Threshold Voltages For Decanano MOSFETs

Final Report

May 2006

TO

USC – Information Sciences Institute

Clinic Team: Luis Avila
Michael Franklin

Faculty Advisor: Darryl Yong
Harvey Mudd College

Consultant: Ellis Cumberbatch
Claremont Graduate University

Liaison: Henok Abebe

Abstract

We calculate the threshold voltage, defined as the gate voltage for which the maximum carrier density reaches the substrate doping level, for a decanano metal oxide semiconductor field effect transistor (MOSFETs) using the density gradient model and matched asymptotic expansions. We also present a novel first integral for the density gradient equations.

Contents

Abstract **iii**

1 Introduction **1**

2 The Classical Problem **5**
2.1 Problem Definition 5
2.2 Threshold Voltage Calculation 8

3 The Quantum Problem **11**
3.1 Problem Definition 11
3.2 The Subthreshold Case 12
3.3 Asymptotics 13
3.4 First Integral 22

Bibliography **25**

Chapter 1

Introduction

The demand for cheaper, faster, more efficient and more powerful computers and electronic devices has led to a relentless downsizing of transistors. According to predictions made by the semiconductor industry, gate lengths (see Figure 2.1) are predicted to shrink to approximately 9 nm by 2016 [1]. Metal oxide semiconductor field effect transistors (MOSFETs) at this decanano (sub 100 nm) scale behave differently than their larger counterparts because quantum mechanical effects become significant.

For many years, the drift-diffusion model (DD) has been widely used to model MOSFETs. Recent experimental evidence shows that the threshold voltage, one of the most important performance characteristics of MOSFETs, is actually higher than the value predicted by this classical (non-quantum) theory at the decanano scale [1, 7].

The distinction between classical and quantum electron densities is shown qualitatively in Figure 1.1. According to quantum mechanics, the electron density is nearly zero at the silicon-insulator (Si/SiO_2) interface and peaks below the interface. This is in contrast to the classical model, where the electron density is greatest at the interface. From a quantum mechanical perspective, the cause of the difference between the classical and quantum electron densities is that when the width of electrical confinement in the region of the Si/SiO_2 interface reaches the order of the de Broglie wavelength, electrons are repelled from the interface [5]. This lowers the density of electrons near the interface, thus requiring a higher voltage to transport these electrons than the classical case (where the density is assumed to be highest at the interface). The discrepancies in the electron density between the classical and quantum cases consequently leads to the disagreement between classical and quantum threshold voltages.

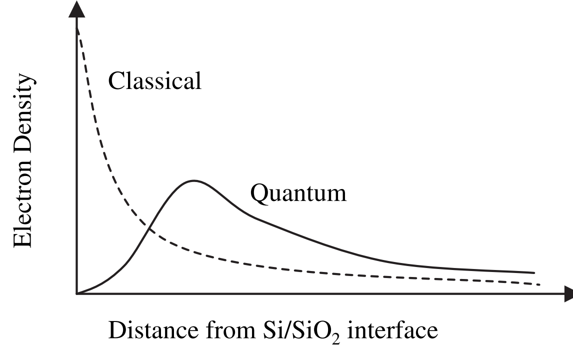

Figure 1.1: Comparison between classical and quantum electron density near the Si/SiO_2 interface, taken from [5].

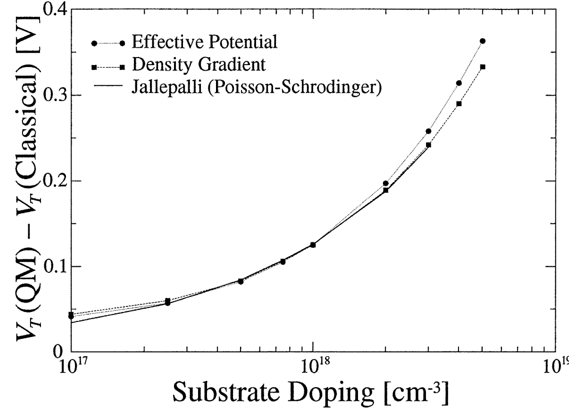

Figure 1.2: Difference between classical and quantum threshold voltages for various levels of doping, taken from [1].

Figure 1.2 shows the difference between classical and quantum threshold voltages increases with substrate doping, N_A. For substrate doping $N_A \approx 10^{17}$ cm^{-3}, the difference between classical and quantum threshold voltages is roughly 0.05 volts [1].

The goal of this paper is to calculate the threshold voltage for decanano MOSFETs using the density gradient (DG) model. Only the cases of constant doping and quantum confinement are considered; tunneling effects are not included. In Chapter 2, we define the governing equations for a classical model of a MOSFET and integrate them to obtain a threshold voltage. In Chapter 3, we present governing equations that incorporate quan-

tum effects using the DG model. We compute composite solutions for the surface potential and carrier density using matched asymptotic expansions and use them to compute a threshold voltage.

Chapter 2

The Classical Problem

2.1 Problem Definition

A cross-sectional view of a MOSFET device is shown in Figure 2.1. The *p*-*n* junction is the primary component in MOSFET devices, which is composed of silicon crystal that has been "doped", meaning one side of the interface is implanted with phosphorus atoms, and the other side with boron atoms. Silicon atoms have four valence electrons, phosphorus has five, and boron has three. Due to electrons' tendency to occupy all valence sites, phosphorus atoms donate electrons to silicon atoms, leaving a density of free electrons n and a static positive charge density N_D. Oppositely, at boron sites, atoms accept electrons from silicon, leaving a negative charge density N_A. This absence of electrons at boron sites, referred to as *holes*, has a density p. The net charge density ρ is

$$\rho = q(p + N_D - n - N_A). \tag{2.1}$$

In an n-channel MOSFET, assuming no recombination and that holes remain in thermal equilibrium, the primary mathematical model describing the motion of electrons and holes are the static drift-diffusion (DD) equations

$$\begin{aligned}
\varepsilon_s \nabla \cdot \mathbf{E} &= -\rho = q(p - n + N) \\
\mathbf{J}_n &= q\mu_n \left(\frac{kT}{q} \nabla n + n\mathbf{E} \right) \\
\nabla \cdot \mathbf{J}_n &= 0 \\
\nabla \psi &= -\mathbf{E} \\
p &= n_i e^{-q\psi/kt},
\end{aligned} \tag{2.2}$$

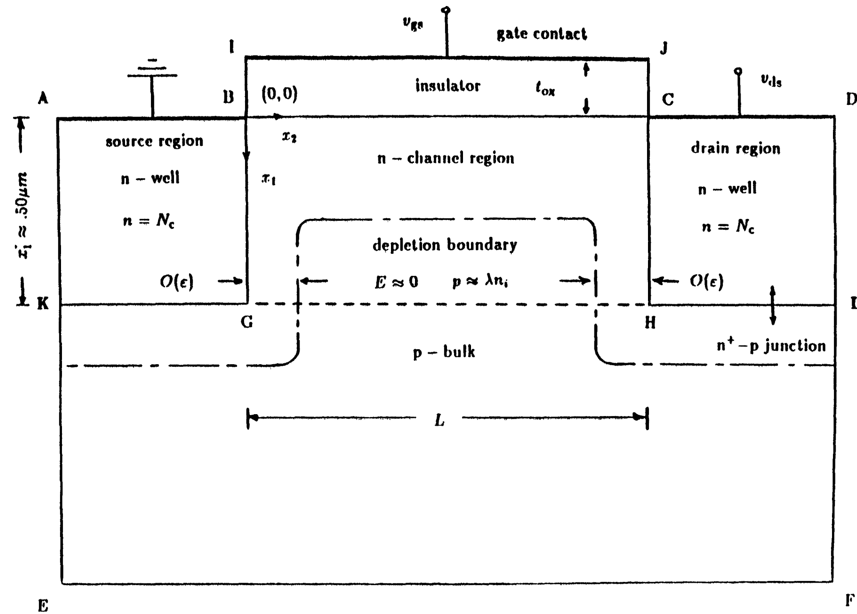

Figure 2.1: Cross sectional view of MOSFET, taken from [15].

where

n, p	are the electron and hole concentrations,
N	is the concentration of selected impurities or dopants,
$\mathbf{J}_n$	is the electron current density,
$\mathbf{E}$	is the electrostatic field,
ψ	is the electrostatic potential,
μ_n	is the electron mobility,
ε_s	is the dielectric constant of the semiconductor,
ρ	is the space charge density,
n_i	is the intrinsic carrier concentration,
q	is the electronic charge,
K	is the Boltzmann's constant,
T	is the constant lattice temperature.

The combination kT/q is called the thermal voltage V_{th}.

This DD model for the transport of electrons and holes has remained the dominant model used in the industry for simulating MOSFET devices. However, the device dimensions are decreasing such that quantum effects are beginning to affect the device behavior, thus becoming a non-negligible

consideration in the mathematical formulation of the problem. The classical DD model provides incorrect results decanano devices [1, 7]. A departure from this classical model is necessary to incorporate quantum effects. An asymptotic analysis of the DD model gives useful insight into the approach of the quantum problem in the Chapter 3.

The classical solution is obtained by a proper rescaling of the variables in (2.2) adopted from [5]. For MOSFETs, the ratio of the maximum channel dopant concentration to the intrinsic level is normally very large, therefore following [15], a large parameter λ is introduced as

$$\lambda = \max\left|\frac{N(x_1)}{n_i}\right| = \frac{N_A}{n_i},$$

where N_A is the substrate doping and n_i is the intrinsic carrier density in silicon. To normalize the electron concentration in the device, the following rescaling is performed

$$\begin{aligned}
&(\psi, \Phi_n) = (w, \phi) V_{th} \ln\lambda, \\
&x_1 = x L_D \left(\frac{2\ln\lambda}{\lambda}\right)^{1/2} \qquad \text{where} \qquad L_D = \left(\frac{kT\varepsilon_{si}}{n_i q^2}\right)^{1/2}, \\
&n = n_i e^{(w-\phi)\ln\lambda}, \\
&p = n_i e^{-w\ln\lambda},
\end{aligned}$$

where V_{th} is the thermal voltage, x_1 is the coordinate perpendicular to the motion of carriers, as shown in Figure 2.1. The quantity L_D is the Debye length. Using this rescaling, the leading-order DD equations are

$$w''(x) = \frac{n-p}{N_A} + 1 = \frac{e^{(w-\phi)\ln\lambda} - e^{-w\ln\lambda}}{\lambda} + 1, \tag{2.3a}$$

$$w - \phi = \frac{1}{\ln\lambda}\ln\left(\frac{n}{n_i}\right). \tag{2.3b}$$

The boundary condition at the Si/SiO_2 interface is

$$\left.\frac{\partial w}{\partial x}\right|_{x=0} = c(w(0) - V_{gs}), \qquad \text{where} \qquad c = \sqrt{\frac{2\ln\lambda}{\lambda}}\frac{\varepsilon_{ox} L_D}{\varepsilon_{si} t_{ox}}$$

is the oxide capacitance, ε_{si} and ε_{ox} are the dielectric constants of silicon and silicon dioxide, t_{ox} is the oxide thickness, and t its rescaled value. The other boundary conditions are

$$w = V_{gs} \quad \text{at} \quad x = -t, \quad \text{and} \quad w \to w_\infty \quad \text{as} \quad x \to \infty.$$

For $\lambda \gg 1$, $w_\infty \sim -1$.

Since $\lambda \gg 1$, each of the terms on the right hand side of (2.3a) can dominate depending on the value of w. According to [5], the solution regimes are

$$\begin{aligned} \textbf{Bulk}: &\quad w \sim -1, \\ \textbf{Depletion}: &\quad -1 < w < 1+\phi, \quad w = \frac{1}{2}x^2 + ax + b, \\ \textbf{Inversion}: &\quad w > 1+\phi, \quad w_{xx} = e^{(w-\phi-1)\ln\lambda}. \end{aligned}$$

Our work is concerned with the subthreshold problem, corresponding to the weak inversion regime [15]. This regime is identified by

$$0 \leq w_s(V_{gs}) \leq 1,$$

where the subscript s is used in this paper to denote the value at $x = 0$.

2.2 Threshold Voltage Calculation

In this section we calculate the classical threshold voltage $V_{T,Cl}$ to give a basis of comparison for the quantum threshold voltage $V_{T,Q}$ calculation in the next chapter. We first compute a first integral of (2.3) by multiplying both sides by w' and integrating to get

$$w' = -2\left[\frac{e^{(w-\phi)\ln\lambda} + e^{-w\ln\lambda}}{\lambda\ln\lambda} + w + K\right]^{1/2}, \tag{2.4}$$

where K is an integration constant. To find K, we allow $x \to \infty$. The boundary condition states $w_\infty \sim -1$, which implies $w'(\infty) = 0$. The constant of integration is then

$$K = -w_\infty - \frac{2e^{-w_\infty\ln\lambda} - \lambda}{\lambda\ln\lambda}. \tag{2.5}$$

On the other hand, the boundary conditions state that at $x = 0$, $w' = c(w(0) - V_{gs})$. Hence, equation (2.4) becomes

$$\frac{c^2(w_s - V_{gs})^2}{2} = \frac{e^{(w_s-\phi)\ln\lambda} + e^{-w_s\ln\lambda}}{\lambda\ln\lambda} + w_s + K. \tag{2.6}$$

Solving equation (2.6) for V_{gs}, we get

$$V_{gs} = w_s + \frac{\sqrt{2}}{c}\left(\frac{e^{(w_s-\phi)\ln\lambda} + e^{-w_s\ln\lambda}}{\lambda\ln\lambda} + w_s + K\right)^{1/2}.$$

The negative root of the equation was chosen to be consistent with the fact that we seek solutions to w that decrease monotonically with x. This is an analytic solution for V_{gs} that is valid for all regimes.

In [15], Ward defines the threshold voltage as the value of V_{gs} for which

$$w_s = 1 + \phi + \frac{\ln(\ln\lambda)}{\ln\lambda}. \tag{2.7}$$

Instead, here we define the threshold voltage as the value of V_{gs} for which the maximum value of the carrier density, matches the substrate doping, N_A. In the classical case, the maximum carrier density occurs at $x = 0$, and the surface potential there is w_s. Therefore, solving

$$\max|n(x)| = n_s = n_i e^{(w_s - \phi)\ln\lambda} = N_A,$$

for w_s yields

$$w_s = 1 + \phi.$$

The threshold voltage is then

$$V_{T,Cl} = 1 + \frac{\sqrt{2}}{c}\left(2 + \frac{1}{\lambda^2 \ln\lambda}\right)^{1/2}. \tag{2.8}$$

The intrinsic carrier density for silicon is $n_i \approx 1.45 \times 10^{10}$ cm^{-3}. A typical value for the substrate doping concentration is $N_A \approx 10^{17}$ cm^{-3}. The permittivity constants of SiO_2 and Si are $\varepsilon_{ox} = 3.9$ and $\varepsilon_{si} = 11.9$ respectively, L_D is the Debye length and the SiO_2 thickness is $t_{ox} = 2$ nm. With these values, the classical threshold voltage is $V_{T,Cl} \approx 1.23589$ volts.

In Chapter 3, we will compare this value with the threshold voltage calculated using the density gradient model.

Chapter 3

The Quantum Problem

3.1 Problem Definition

This section presents the calculations when quantum mechanical effects are included in the governing equations by means of the density gradient (DG) model. After appropriate scaling, the reduced system of differential equations looks very similar to the classical DD model, except for a quantum correction term [5]. In the DD model, the electron and hole drift potentials are $\phi_n = \phi_p = \phi$, but according to the DG model, ϕ_n and ϕ_p are given by

$$\phi_n = \phi + \phi_{qn}, \qquad \phi_{qn} = 2b_n \frac{\nabla^2 \sqrt{n}}{\sqrt{n}}, \qquad b_n = \frac{\hbar^2}{4r_n m_n q},$$

$$\phi_p = \phi + \phi_{qp}, \qquad \phi_{qp} = 2b_p \frac{\nabla^2 \sqrt{p}}{\sqrt{p}}, \qquad b_p = \frac{\hbar^2}{4r_p m_n q},$$

where n and p are the electron and hole densities respectively, $\hbar$ is Planck's constant, r is a fitting parameter, m is the mass of the electron and q is its charge. The quantum corrections ϕ_{qn} and ϕ_{qp} are derived from the Schrödinger equation, based on the finite curvature (energy) and strict continuity of wavefunctions (in fact, the DG model forbids discontinuities in the carrier density profile) [3].

In the DG model, a microscopic quantum description is used in regions with dominant quantum effects, and a macroscopic (fluid-type) model is employed in subregions where collisional effects are expected to be dominant [2]. In the expression for ϕ_n, the correction ϕ_{qn} to the quasi-Fermi potential is derived using Boltzmann statistics. Consequently, a comparison of our results with the results obtained by SCHRED (`www.nanohub.org`) is not possible, because according to the theoretical documentation on the

software, both electrons and holes are treated classically and assuming general Fermi-Dirac statistics [6].

With the quantum corrections to the DD model, the governing equations become

$$\frac{d^2w}{dx^2} = \frac{n-p}{N_A} + 1, \tag{3.1a}$$

$$w - \phi = \frac{1}{\ln\lambda}\ln\left(\frac{n}{n_i}\right) - \frac{\lambda\beta^2}{(\ln\lambda)^2}\frac{1}{\sqrt{n}}\frac{d^2\sqrt{n}}{dx^2}, \tag{3.1b}$$

where

$$\beta^2 = \frac{2b_n}{V_{th}L_D^2}.$$

The quantum correction does not affect the boundary conditions for the potential at the Si/SiO_2 interface, but using the well-accepted boundary condition for the electron density, the boundary conditions for (3.1) are

$$n(0) = 0, \quad w(0) = w_s, \quad \text{and} \quad w(\infty) = w_\infty \sim -1,$$

as well as the Robin boundary condition

$$\left.\frac{dw}{dx}\right|_{x=0} = c(w_s - V_{gs}), \tag{3.2}$$

as in Chapter 2.

3.2 The Subthreshold Case

The subthreshold case corresponds to the weak inversion regime, meaning $0 \leq w_s(V_{gs}) \leq 1$. In this case, the dominant contribution to the space charge density near the interface arises from the immobile acceptor ions, N_A [15]. This can be justified by looking at the hole concentration

$$p(x) = n_i e^{-w\ln\lambda} \ll 1 \qquad \text{if} \qquad 0 \leq w_s \leq 1,$$

and noting that in the weak inversion regime, the electron density $n(x)$ is negligible because it is much less than the doping level, i.e. $n(x) \ll N_A$. Thus, the system of equations for the subthreshold case becomes

$$\frac{d^2w}{dx^2} = 1, \tag{3.3a}$$

$$w - \phi = \frac{1}{\ln\lambda}\ln\left(\frac{n}{n_i}\right) - \frac{\lambda\beta^2}{(\ln\lambda)^2}\frac{1}{\sqrt{n}}\frac{d^2\sqrt{n}}{dx^2}. \tag{3.3b}$$

We will determine the potential and electron density using matched asymptotic expansions (MAEs). This is done by introducing a quantum inner layer near the interface governed by (3.3) and an outer depletion layer governed by the classical model (2.3), and properly matching them.

3.3 Asymptotics

Due to rapid changes in the potential near the Si/SiO_2 interface, an asymptotic approach is taken to find the solution to (3.3). In the MAE technique, approximate solutions to the differential equations, valid in adjacent but overlapping regions, are blended together by suitably matching integration constants, resulting in a composite solution valid over the whole region of interest [5]. In the region near the interface, the quantum inner layer, the device behavior is drastically different than in the classical case. Solutions in this layer are obtained by formal expansions in a small parameter, ε. Following [5], the quantum inner layer independent variable scaling is

$$X = \frac{x}{\varepsilon} \qquad \text{where} \qquad \varepsilon^2 = \frac{\lambda\beta^2}{2\ln\lambda}.$$

The dependent variables of (3.3) are also expanded formally in powers of ε as

$$(w, T, Y) = (W_0, T_0, Y_0) + \varepsilon(W_1, T_1, Y_1) + \mathcal{O}(\varepsilon^2),$$

where it is convenient, as in [5], to use the following rescaled variables

$$T = \sqrt{\frac{n}{n_i}} \qquad \text{or} \qquad Y = \frac{1}{\ln\lambda}\ln\left(\frac{n}{n_i}\right). \tag{3.4}$$

When the scaled independent variable X is substituted into (3.3a), the equation reads

$$\frac{d^2 w}{dX^2} = \varepsilon^2 \qquad \text{thus} \qquad \frac{d^2}{dX^2}(W_0 + \varepsilon W_1 + \mathcal{O}(\varepsilon^2)) = \varepsilon^2.$$

Equation (3.3b) can be rewritten in terms of either T or Y as

$$\frac{1}{T}\frac{d^2 T}{dX^2} - \ln T + \frac{\ln\lambda}{2}(w - \phi) = 0, \tag{3.5a}$$

$$\frac{d^2 Y}{dX^2} + \frac{1}{2}\ln\lambda\left(\frac{dY}{dX}\right)^2 + w - \phi - Y = 0. \tag{3.5b}$$

The boundary condition is also written in terms of the scaled variables as

$$\frac{d}{dX}(W_0 + \varepsilon W_1 + \mathcal{O}(\varepsilon^2))\bigg|_{X=0} = \varepsilon c(W_{0s} - V_{gs}). \tag{3.6}$$

The value of the potential at $x = 0$ in this paper is defined as $w_s \equiv W_{0s}$. Separating in orders of ε and using the boundary condition (3.6) to solve the resulting systems, the inner solution $W(X) = W_0(X) + \varepsilon W_1(X) + \mathcal{O}(\varepsilon^2)$ is

$$W(X) = W_{0s} + \varepsilon c(W_{0s} - V_{gs})X + \mathcal{O}(\varepsilon^2). \tag{3.7}$$

This quantum inner layer solution represents the device behavior close to the interface, on the order of the reference length, $L_D\sqrt{\ln\lambda/\lambda}$, which has a value of 123 nm for $\lambda = 10^6$ [5]. Equation (3.5b) will describe the quantum potential's coupling to the electron density in this layer.

Proceeding the quantum inner layer is the depletion outer layer, because in the subthreshold case, the device has not yet gone into inversion, thus no inversion layer is present. The equations for the outer depletion layer are

$$\frac{d^2 w}{dx^2} = 1, \tag{3.8a}$$

$$n(x) = n_i e^{(w-\phi)\ln\lambda}. \tag{3.8b}$$

Expanding the depletion potential and boundary condition using $w(x) = w_0(x) + \varepsilon w_1(x) + \mathcal{O}(\varepsilon^2)$ and grouping into orders of ε, we arrive at the following depletion layer solution:

$$w(x) = \frac{1}{2}x^2 + (a_0 + \varepsilon a_1)x + (b_0 + \varepsilon b_1) + \mathcal{O}(\varepsilon^2). \tag{3.9}$$

The coefficients $(a, b) = (a_0, b_0) + \varepsilon(a_1, b_1) + \mathcal{O}(\varepsilon^2)$ are determined by matching the depletion potential on the left with the quantum layer, and on the right with a transition layer that is used to blend the solution with the bulk. To match the depletion layer with the quantum layer, an intermediate variable is introduced:

$$x_\eta = \frac{x}{\eta(\varepsilon)}, \qquad \text{where} \qquad \varepsilon \ll \eta(\varepsilon) \ll 1.$$

Verifying that

$$\lim_{\varepsilon\to 0}\left|\frac{(W_0(x_\eta) + \varepsilon W_1(x_\eta)) - (w_0(x_\eta) + \varepsilon w_1(x_\eta))}{\varepsilon}\right| = 0,$$

we gather the following information on the depletion layer solution:

$$a_0 = c(W_{0s} - v_{gs}), \qquad b_0 = W_{0s}, \qquad b_1 = 0.$$

No information on the coefficient a_1 can be extracted by the matching with the quantum layer, so this information comes by matching the depletion layer with the bulk solution,

$$w_b(x) = -1 + \mathcal{O}(1/\lambda^2 \ln \lambda).$$

The matching of the depletion layer with the bulk is done in [15] by introducing a transition layer about some unknown depth x_d (referred to as the depletion width) where the proper scalings are

$$x_t = (x - x_d)(\ln \lambda)^{1/2} \qquad \text{and} \qquad w = w_t(x_t) = -1 + \frac{h_0(x_t)}{\ln(\lambda)}.$$

In terms of these new scaled variables, the transition layer equation for h_0 is

$$\frac{d^2 h_0}{dx_t^2} = 1 - e^{-h_0},$$

where $h_0(\infty) = 0$ is needed to match to the bulk. It is not possible to explicitly integrate this equation, however a first integral provides the implicit expression

$$-\sqrt{2} x_t = \int_1^{h_0} (e^{-y} + y - 1)^{-1/2}\, dy.$$

Analogous to the matching of the depletion layer with the quantum layer, we define an intermediate variable

$$x_\eta = \frac{x - x_d}{\eta(\lambda)} \qquad \text{where} \qquad \frac{1}{(\ln \lambda)^{1/2}} \ll \eta(\lambda) \ll 1.$$

Expanding the implicit transition layer solution as $x_t \to \infty$ or alternatively as $h_0 \to \infty$ provides

$$w_t(x_\eta) \sim \frac{1}{2}\eta^2 x_\eta^2 - \frac{k \eta x_\eta}{\sqrt{2 \ln \lambda}} + \frac{1}{\ln \lambda}\left(\frac{k^2}{4} + 1\right) - 1,$$

where

$$k = \int_1^\infty [(y-1)^{-1/2} - (e^{-y} + y - 1)^{-1/2}]\, dy \approx 0.81785.$$

See [15] for more details describing this numerical result. Expanding the depletion solution (3.9) using $w(x_\eta) = w_0(x_\eta) + \varepsilon w_1(x_\eta) + \mathcal{O}(\varepsilon^2)$ in terms of the intermediate variable gives

$$w(x_\eta) = \frac{1}{2}(\eta x_\eta + x_d)^2 + c(W_{0s} - V_{gs})(\eta x_\eta + x_d) + \varepsilon a_1(\eta x_\eta + x_d) + W_{0s} + \mathcal{O}(\varepsilon^2).$$

Comparing the depletion and transition solutions to $\mathcal{O}(1)$ and $\mathcal{O}(\eta)$ gives the following equations

$$\begin{aligned}
\mathcal{O}(1): \quad & \frac{1}{2}x_d^2 + \left(c(W_{0s} - V_{gs}) + \varepsilon a_1\right) x_d - \frac{1}{\ln \lambda}\left(\frac{k^2}{4} + 1\right) + W_{0s} + 1 = 0, \\
\mathcal{O}(\eta): \quad & x_d + c(W_{0s} - V_{gs}) + \varepsilon a_1 + \frac{k}{\sqrt{2 \ln \lambda}} = 0.
\end{aligned}$$

Solving this system of equations for a_1 and x_d gives

$$\begin{aligned}
a_1 &= -\frac{1}{\varepsilon}\left[\sqrt{2}\left(1 + W_{0s} - \frac{1}{\ln \lambda}\right)^{1/2} + c(W_{0s} - V_{gs})\right] \\
x_d &= \sqrt{2}\left(1 + W_{0s} - \frac{1}{\ln \lambda}\right)^{1/2} - \frac{k}{\sqrt{2 \ln \lambda}}.
\end{aligned}$$

Thus, we are now able to write the full depletion layer solution $w(x) = w_0(x) + \varepsilon w_1(x) + \mathcal{O}(\varepsilon^2)$ as

$$w(x) = \frac{1}{2}x^2 - \sqrt{2}\left(1 + W_{0s} - \frac{1}{\ln \lambda}\right)^{1/2} x + W_{0s} + \mathcal{O}(\varepsilon^2). \tag{3.12}$$

This expression for the depletion layer potential agrees with the results obtained in the weak inversion-depletion analysis done in [15]. From this expression we notice that the expansion breaks down near flatband where $w_s = -1 + \mathcal{O}(1/\ln \lambda)$ [15]. At this point, it is possible to use the boundary condition (3.2) for the depletion potential (3.12) to derive an expression for surface potential W_{0s} in terms of applied gate voltage V_{gs}. The boundary condition states that

$$\left.\frac{dw}{dx}\right|_{x=0} = c(W_{0s} - V_{gs}),$$

thus,

$$-\sqrt{2}\left(1 + W_{0s} - \frac{1}{\ln \lambda}\right)^{1/2} = c(W_{0s} - V_{gs}).$$

Solving the above expression for $W_{0s}(V_{gs})$ gives

$$W_{0s}(V_{gs}) = V_{gs} + \frac{1}{c^2} - \frac{\sqrt{2}}{c}\left(\frac{1}{2c^2} + 1 + V_{gs} - \frac{1}{\ln\lambda}\right)^{1/2}, \tag{3.13}$$

which gives an explicit value for the surface potential given any gate voltage. Analogously, solving the classical equation (2.3a) in the depletion region gives

$$w_s(V_{gs}) = \frac{1}{c^2} + V_{gs} - \frac{\sqrt{2}}{c}\left(\frac{1}{2c^2} + 1 + V_{gs}\right)^{1/2}. \tag{3.14}$$

The next task is to determine a valid electron density $n(x)$ throughout the full region of interest. The equations (3.5) relating the quantum layer potential and electron density is independent of the solution regime being examined, and consequently the solution is the same as in [5] where the strong inversion case is examined. The solution is obtained by substituting the expansion $T = T_0 + \varepsilon T_1 + \mathcal{O}(\varepsilon^2)$ into (3.5a) and taking $\mathcal{O}(1)$ terms, giving

$$\frac{d^2 T_0}{dX^2} - T_0 \ln(T_0) + \frac{\ln\lambda}{2}(W_0 - \phi)T_0 = 0,$$

where from (3.4) we can write

$$T_0 = \exp\left(Y_0 \ln\lambda/2\right) \qquad \text{and} \qquad \tau_{0s} \equiv T_0(\infty) = \exp\left((W_{0s} - \phi)\ln\lambda/2\right).$$

Using these expressions with the quantum inner solution $W_0(X) = W_{0s}$ and boundary condition, this $\mathcal{O}(1)$ expression can be written as

$$\frac{d^2 S_0}{dX^2} = S_0 \ln(S_0) \qquad \text{where} \qquad S_0 = \frac{T_0}{\tau_{0s}}.$$

The solution to this equation is available only in implicit form, but an approximation that yields similar asymptotic results is

$$S_0(X) = \tanh\left(X/2\right),$$

which has the required behavior at $X \ll 1$ and asymptotic decay for $X \gg 1$ [5]. From this approximation, the expression for the quantum electron density can be expressed in terms of Y as

$$Y_0(X) = \frac{2}{\ln\lambda}\ln\left(\tau_{0s}\tanh\left(X/2\right)\right) = W_{0s} - \phi + \frac{2}{\ln\lambda}\ln\left(\tanh\left(X/2\right)\right). \tag{3.15}$$

In the depletion layer, the electron density behaves classically, with a straightforward expression given by (3.8b).

To correctly represent the composite solution throughout the entire region, the two separately calculated solutions are added together and the common terms are subtracted out. Following [5],

$$Y = \frac{1}{\ln \lambda} \ln\left(\frac{n}{n_i}\right) = w_0 + \varepsilon w_1 + Y_0 - W_{0s} + \cdots .$$

Thus, using this expression and solving for the electron density $n(x)$, the result is given by

$$n(x) = n_i \exp\left[(w(x) + Y_0(x) - W_{0s}) \ln \lambda\right], \tag{3.16}$$

where $w(x)$ and $Y_0(x)$ are given respectively by (3.12) and (3.15), and W_{0s} is the common term subtracted out.

The threshold voltage is defined in our work as the value of the gate voltage V_{gs} that, when applied to the gate, raises the maximum carrier density $n(x)$ to the doping level N_A. In the classical case, the carrier density is highest at the interface, whereas in the quantum case, the carrier density achieves a maximum value at a distance from the interface. It is desirable to find an expression for the value $x = x^*$ which maximizes the value of $n(x)$ given in (3.16). In other words, we seek to find $\max|n(x)| = n(x^*)$. We notice that the expression (3.16) achieves a maximum value when the argument of the exponent achieves a maximum, i.e.

$$\max|n(x)| \qquad \text{achieved at} \qquad \max|w(x) + Y_0(x) - W_{0s}|.$$

Thus, we are seeking the maximum value of the expression

$$\frac{1}{2}x^2 - \sqrt{2}\left(1 + W_{0s} - \frac{1}{\ln \lambda}\right)^{1/2} x + \frac{2}{\ln \lambda} \ln\left(\tau_{0s} \tanh\left(\frac{x}{2\varepsilon}\right)\right).$$

The maximum value is found by taking the derivative with respect to x and setting it equal to zero, which means

$$x - \sqrt{2}\left(1 + W_{0s} - \frac{1}{\ln \lambda}\right)^{1/2} + \frac{2}{\varepsilon \ln \lambda \sinh(x/\varepsilon)} = 0.$$

The hyperbolic sine can be written as

$$\sinh(x/\varepsilon) = \frac{e^{x/\varepsilon} - e^{-x/\varepsilon}}{2} \approx \frac{e^{x/\varepsilon}}{2},$$

when $x/\varepsilon \gg 1$. This yields an accurate approximation for the derivative, thus the equation we wish to solve becomes

$$x - \sqrt{2}\left(1 + W_{0s} - \frac{1}{\ln\lambda}\right)^{1/2} + \frac{4}{\varepsilon \ln\lambda} e^{-x/\varepsilon} = 0.$$

Solving this equation for x^* involves using the Lambert W function [9], and gives the following expression

$$x^* = \overline{K} + \varepsilon \text{LambertW}\left(-\frac{4}{\varepsilon^2 \ln\lambda} \exp\left(-2\overline{K}/\varepsilon\right)\right),$$

where

$$\overline{K} = \sqrt{2}\left(1 + W_{0s} - \frac{1}{\ln\lambda}\right)^{1/2}.$$

Care must be taken when selecting the appropriate branch of the Lambert W function to give the correct value of x^*. At this point, the threshold voltage $V_{T,Q}$ is the value of V_{gs} which makes $n(x^*; V_{gs}) = N_A$; in other words

$$n_i \exp\left[\left(w(x^*; V_{T,Q}) + Y_0(x^*; V_{T,Q}) - W_{0s}(V_{T,Q})\right) \ln\lambda\right] = N_A,$$

where $W_{0s}(V_{T,Q})$ is given by (3.13). Unlike the classical threshold voltage $V_{T,Cl}$ given in (2.8), this expression cannot be solved explicitly for $V_{T,Q}$. However, for the same parameter values used in the classical threshold voltage calculation, solving numerically yields a threshold voltage of $V_{T,Q} \approx$ 1.30465 volts. As expected, the quantum threshold voltage is higher than the classical threshold voltage. The electron density profiles for both classical and quantum models are shown in Figures 3.1 and 3.2. The comparison of the classical and quantum threshold voltages for a range of substrate doping is shown in Figures 3.3 and 3.4.

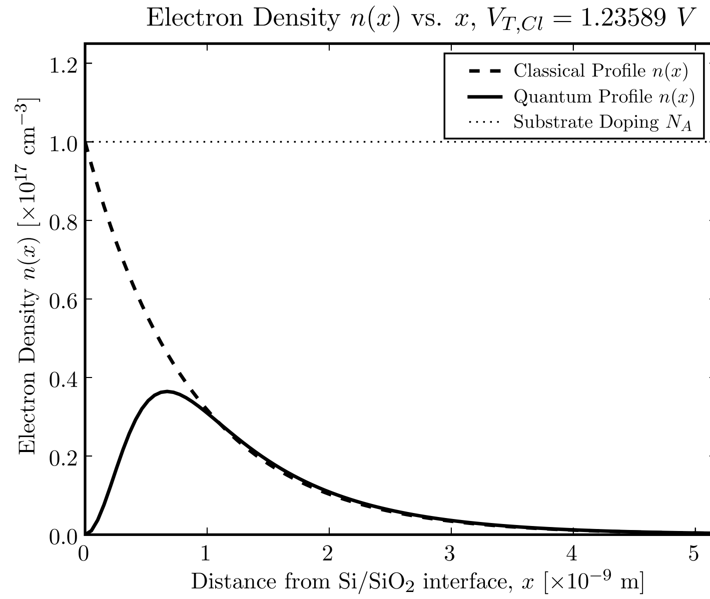

Figure 3.1: Electron density profiles at classical threshold voltage, $V_{T,Cl}$.

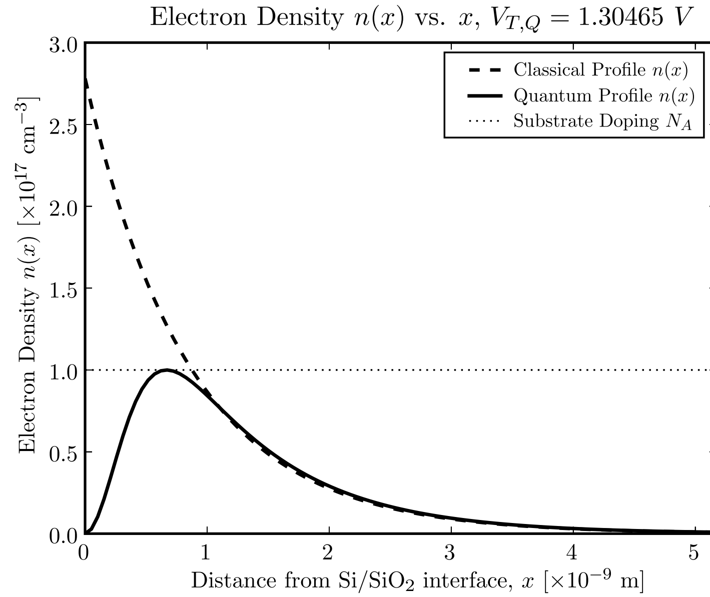

Figure 3.2: Electron density profiles at quantum threshold voltage, $V_{T,Q}$.

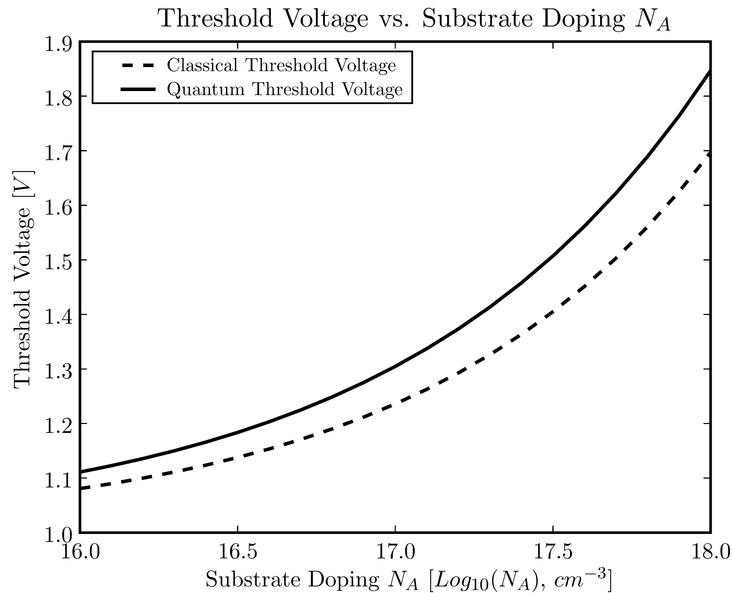

Figure 3.3: Threshold voltage vs N_A comparison between classical and quantum models.

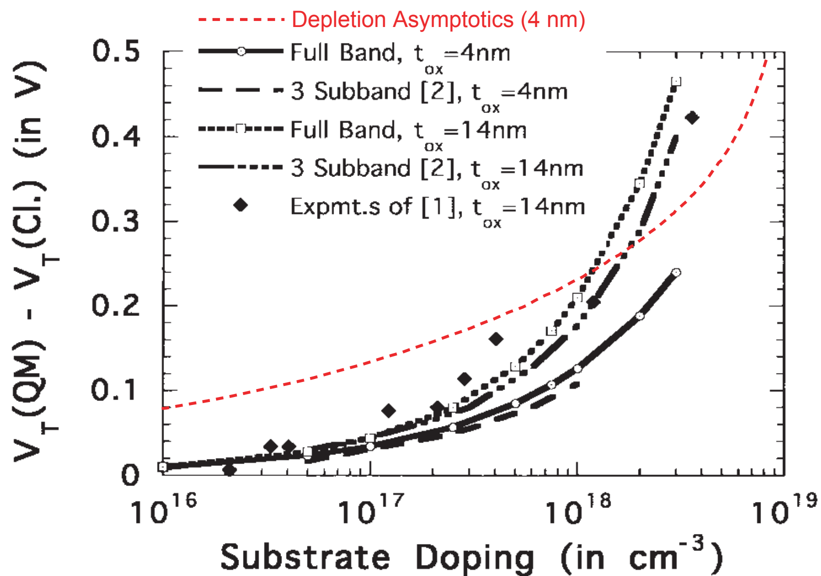

Figure 3.4: Difference between classical and quantum threshold voltages as a function of substrate doping; Poisson-Schrödinger classical results taken from [7], whose authors define threshold voltage as the gate voltage at which the net inversion sheet charge is 10^{-3} times the net depletion charge.

3.4 First Integral

An interesting calculation can be done in which the governing equations in the quantum case (3.1) can be integrated once to give an exact expression for $w_s(V_{gs})$. This is done by first making the substitution $a = \sqrt{n}$ to simplify the equations, which gives

$$w'' = \frac{a^2 - p}{N_A} + 1, \tag{3.17a}$$

$$w - \phi = \frac{1}{\ln \lambda} \ln \left(\frac{a^2}{n_i} \right) - \frac{\lambda \beta^2}{(\ln \lambda)^2} \frac{a''}{a}, \tag{3.17b}$$

where $p = n_i \exp(-w \ln \lambda)$. Multiplying (3.17a) by w' gives

$$a^2 w' = N_A (w' w'' - w') + n_i e^{-w \ln \lambda} w', \tag{3.18}$$

and multiplying (3.17b) by aa' gives

$$aa'w - \left[\frac{a^2 \phi}{2} \right]' = \frac{1}{2 \ln \lambda} \left[a^2 \left(2 \ln \left(\frac{a}{\sqrt{n_i}} \right) - 1 \right) \right]' - \frac{\lambda \beta^2}{(\ln \lambda)^2} \left[\frac{(a')^2}{2} \right]'. \tag{3.19}$$

Finally, we use the identity

$$(a^2 w)' = 2aa'w + a^2 w'$$

to combine (3.18) and (3.19) into a single equation in which every term can be integrated once. After integrating, we obtain

$$\frac{1}{2} \left[a^2 w - N_A \left(\frac{1}{2} (w')^2 - w \right) + \frac{n_i}{\ln \lambda} e^{-w \ln \lambda} \right] - \frac{a^2 \phi}{2} = \frac{a^2}{2 \ln \lambda} \left(2 \ln \left(\frac{a}{\sqrt{n_i}} \right) - 1 \right) - \frac{\lambda \beta^2}{(\ln \lambda)^2} \frac{(a')^2}{2} + \frac{K}{2}, \tag{3.20}$$

where K is an integration constant that is determined using the limiting values of w and a as $x \to \infty$. The constant works out to be

$$\frac{K}{N_A} = w_\infty + \frac{1}{\ln \lambda} \left[\frac{2e^{-w_\infty \ln \lambda}}{\lambda} - 1 \right].$$

Now we let $x = 0$ and use the boundary conditions $a(0) = 0$, $w(0) = w_s$, $w'(0) = c(w_s - V_{gs})$ to get

$$c(w_s - V_{gs}) = -\sqrt{2} \left(w_s + \frac{e^{-w_s \ln \lambda}}{\lambda \ln \lambda} + \frac{\lambda \alpha^2 \beta^2}{N_A (\ln \lambda)^2} - \frac{K}{N_A} \right)^{1/2},$$

where $\alpha \equiv a'(0)$. This equation is only valid at the Si/SiO$_2$ interface at $x = 0$, and similar to (3.14) and (3.13), it relates the surface potential and gate voltage. The equation is valid for any working regime of the device, since we did not neglect n, p, or 1 on the right hand side of (3.1a) in its calculation. Using Ward's definition of the threshold voltage as the gate voltage when $w_s = 1 + \phi + \ln(\ln\lambda)/\ln\lambda$, this effectively reduces the problem of determining the threshold voltage to the problem of determining α. Any other definition of threshold voltage will require an alternate approach to acquire a solution.

One method of computing α without requiring the complete analytic solution to the ODEs (3.1a) and (3.1b) is to use an asymptotic expansion in x to determine w and a in a quantum boundary layer. In [5], Cumberbatch, Uno and Abebe use matched asymptotics to find a uniform asymptotic solution for w and a in the case of inversion, $w_s \geq 1$. Since we only need the value of α, only the solution in this quantum boundary layer is necessary. Even though their results were for the strong inversion case, by using the first term of the asymptotic solution in this quantum layer we found that

$$\alpha = a'(0) \approx \frac{1}{\varepsilon}\sqrt{\frac{n_i \lambda \ln\lambda}{2}},$$

which produces a threshold voltage identical to that obtained for the classical case in equation (2.8). Similar results could be performed to approximate α in the depletion case.

Bibliography

[1] A. Asenov, A. R. Brown, and J. R. Watling, *Quantum corrections in the simulation of decanano MOSFETs*, Solid-State Electronics (2003), no. 33, 1141–1145.

[2] A. El Ayyadi and A. Jüngel, *Semiconductor simulations using a coupled quantum drift-diffusion schrödinger-poisson model*, SIAM J. Appl. Math **66** (2005), no. 2, 554–572.

[3] B. A. Biegel, M. G. Ancona, C. S. Rafferty, and Z. Yu, *Efficient multi-dimensional simulation of quantum confinement effects in advanced MOS devices*, Tech. report, NASA Advanced Superconducting Division, August 2004, NAS-04-008, accessed from `http://www.nas.nasa.gov/News/Techreports/2004/PDF/nas-04-008.pdf`.

[4] B. A. Biegel, C. S. Rafferty, Z. Yu, M. G. Ancona, and R. W. Dutton, *Simulation of ultra-small MOSFETs using a 2-D quantum-corrected drift-diffusion model*, Proceedings of the Gigascale Integration Technology Symposium, 35th Annual Technical Meeting, Society of Engineering Science (SES35), September 1998, pp. 53–64.

[5] E. Cumberbatch, S. Uno, and H. Abebe, *Nano-scale MOSFET device modeling with quantum effects*, European Journal of Applied Mathematics (2006), to appear.

[6] S. Hassan, *Schred 2.1 tutorial*, 2003, downloaded from `http://www.nanohub.org/index.php?option=com_docman&task=docclick&Itemid=69&bid=132`, Schred available at `http://www.nanohub.org/simulation_tools/schred_tool_information`.

[7] S. Jallepalli, J. Bude, W. K. Shih, M. R. Pinto, C. M. Maziar, and Jr. A. F. Tasch, *Electron and hole quantization and their impact on deep sub-*

micronsilicon p- and n-MOSFET characteristics, IEEE Trans. Electron Devices **44** (1997), no. 2, 297–303.

[8] Y. Ohkura, *Quantum effects in Si n-MOS inversion layer at high substrate concentration*, Solid-State Electronics (1990), no. 33, 1581–1585.

[9] A. Ortiz-Conde, F. J. Garciá Sáchez, and M. Guzmán, *Exact analytical solution of channel surface potential as an explicit function of gate voltage in undoped-body MOSFETs using the lambert w function and a threshold voltage definition therefrom*, Solid-State Electronics **47** (2003), 2067–2074.

[10] S. Selberherr, *Analysis and simulation of semiconductor devices*, Springer-Verlag, 1984.

[11] S. M. Sze, *Physics of semiconductor devices*, 2nd ed., John Wiley and Sons, 1981.

[12] Y. Taus and T. H. Ning, *Fundamentals of modern VLSI devices*, Cambridge University Press, 1998.

[13] S. Uno, H. Abebe, and E. Cumberbatch, *Analytical descriptions of inversion layer quantum effects using a density gradient model and singular perturbation theory*, IEEE Trans. Electron Devices (2006), submitted February 2006.

[14] ———, *Analytical formulae of quantum-mechanical electron density in inversion layer in planar MOSFETs*, Proceedings of the Third International Workshop on Compact Modeling, January 2006, downloaded from `http://www.isi.edu/~abebeh/Uno2006IWCMManuscript_1.pdf`.

[15] M. J. Ward, F. M. Odeh, and D. S. Cohen, *Asymptotic methods for metal oxide semiconductor field effect transistor modeling*, SIAM J. Appl. Math **50** (1990), no. 4, 1099–1125.